Phase Transitions and Distortion of $[BiCl_6]^{3-}$ Octahedra in $(C_3H_5NH_3)_3[BiCl_6]$ – DSC and Single-Crystal X-Ray Diffraction Studies

Bartosz Zarychta, Maciej Bujak, and Jacek Zaleski

Institute of Chemistry, University of Opole, Oleska 48, 45-052 Opole, Poland

Reprint requests to Prof. J. Zaleski. Fax: (+48)-77-4410741. E-mail: zaleski@uni.opole.pl

The DSC diagram of tris(allylammonium) hexachlorobismuthate(III), $(C_3H_5NH_3)_3[BiCl_6]$, revealed three anomalies at 152, 191 and 299 K. The structure of the salt was determined at 200 and 315 K, below and above the high-temperature phase transition at 299 K. In both phases the crystals are monoclinic. At 200 K the space group is $C2/c$ whereas at 315 K it is $C2/m$. The structures, at both temperatures, are composed of $[BiCl_6]^{3-}$ octahedra and allylammonium cations. The organic and inorganic moieties are attracted to each other by a network of the N–H...Cl hydrogen bonds. The relationship between corresponding parameters of the unit cells has been found. The phase transition at 299 K, of the order-disorder type, is attributed to the ordering of one non-equivalent allylammonium cation in the low-temperature phase.

Key words: Chlorobismuthates(III), Allylammonium Cation, Phase Transition, Disorder, Octahedral Distortion

1. Introduction

Chlorobismuthates(III) with organic cations have been the subject of intense investigations for the last few years [1–3]. These organic-inorganic salts may be obtained in a reaction of the chosen organic compound and basic bismuth(III) carbonate in an aqueous solution of hydrochloric acid. Anionic substructures of chlorobismuthates(III) are formed of distorted $[BiCl_6]^{3-}$ octahedra, which are either isolated or connected with each other by bridging chlorine atoms forming more complicated arrays, like polyanionic one-, two- or three-dimensional nets. The inorganic octahedra may share corners, edges or faces. The organic cations, located between the anions, are usually connected to the chlorine ligands by N–H...Cl and C–H...Cl hydrogen bonds [4]. The characteristic feature of these compounds is the molecular dynamics of the cations. On decreasing the temperature molecular motions of cations usually are frozen. This may lead to one or more phase transitions. Among chlorobismuthates(III) those with isolated bioctahedral $[Bi_2Cl_{11}]^{5-}$ units are the most interesting owing to their polar character [5, 6].

In this paper we report the preparation, structure and phase transitions in tris(allylammonium) hexachlorobismuthate(III).
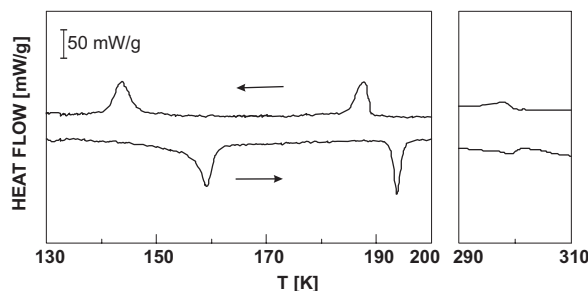

Fig. 1. DSC diagram of $(C_3H_5NH_3)_3[BiCl_6]$.

2. Results and Discussion

2.1. Thermoanalytical studies

The phase transitions in tris(allylammonium) hexachlorobismuthate(III) were determined from the shape of a DSC plot. The calorimetric analysis was followed by the TGA measurement, which has shown that the crystals of the title compound start to decompose above *ca.* 410 K. The DSC studies revealed three distinct thermal anomalies at 152, 191 and 299 K (Fig. 1), which are well reproducible and reversible. The relatively sharp peaks and the values of the thermal hysteresis (9 and 3 K for the transitions at 152 and 191 K, respectively) of the anomalies below room temperature suggest that both low-temperature phase transitions

Table 1. Transitions temperature, enthalpy, entropy and character of the phase transitions in tris(allylammonium) hexachlorobismuthate(III) crystals.

T [K]	ΔH [kJ·mol^{-1}]	ΔS [J·mol^{-1}·K^{-1}]	Order of phase transition
152	1.48	9.71	first
191	0.96	5.01	first
299	0.18	0.60	first or second

Table 2. Crystal data and structure determination for [C$_3$H$_8$N]$_3$[BiCl$_6$] at 315 and 200 K.

	315 K	200 K
Empirical formula	C$_9$H$_{24}$N$_3$BiCl$_6$	
Formula weight	595.99	
Colour	yellowish	
Crystal size [mm^3]	0.1 × 0.15 × 0.15	
Crystal system	monoclinic	
Space group	$C2/m$	$C2/c$
Unit cell dimensions [Å, °]		
a	22.758(1)	27.605(2)
b	7.882(1)	7.835(1)
c	12.290(1)	22.465(2)
β	108.64(1)	122.47(1)
Volume [Å^3]	2088.9(4)	4099.3(8)
Z	4	8
Temperature [K]	315(1)	200(1)
Density (calculated) [g·cm^{-3}]	1.847	1.899
Absorption coefficient [mm^{-1}]	9.198	9.375
Wavelength [Å]	0.71073	
Scan type	ω-scan	
Number of reflections used for cell determination	4843	12386
θ Range for data collection [°]	3.40 – 24.99	3.18 – 25.00
Index ranges	$-27 \leq h \leq 27$	$-32 \leq h \leq 32$
	$-9 \leq k \leq 9$	$-8 \leq k \leq 9$
	$-14 \leq l \leq 14$	$-26 \leq l \leq 26$
Reflections collected/unique	4843/1911	12386/3600
Refinement method	Full-matrix least squares on F^2	
Data/parameters	1911/140	3600/237
Goodness of fit	1.002	0.857
Final R indices ($I > 2\sigma(I)$)	$R_1 = 0.0275$	$R_1 = 0.0265$
	$wR_2 = 0.0573$	$wR_2 = 0.0434$
R Indices (all data)	$R_1 = 0.0334$	$R_1 = 0.0415$
	$wR_2 = 0.0592$	$wR_2 = 0.0458$
Largest diff. peak and hole [e·Å^{-3}]	-0.65 and 0.76	-0.90 and 0.94

are of the first order. In contrast, the high-temperature transformation could be considered as the second order one. The transition temperatures, enthalpies, entropies and character of the detected phase transitions are depicted in Table 1.

2.2. X-ray studies

X-ray single-crystal studies have been undertaken to obtain further information about the structural changes

Table 3. Final atomic coordinates and equivalent isotropic displacement parameters (Å$^2 \cdot 10^3$) for non-H atoms for the (C$_3$H$_5$NH$_3$)$_3$[BiCl$_6$] structure at 315 K ($C2/m$).

Atom	x	y	z	U_{eq}
Bi1	0.6731(1)	1/2	0.7040(1)	0.0506(1)
Cl1	0.5825(1)	0.2598(2)	0.6307(2)	0.0861(5)
Cl2	0.7569(1)	0.7451(2)	0.7648(2)	0.0993(6)
Cl3	0.6791(1)	0.5458(4)	0.4853(2)	0.069(1)
Cl4	0.6621(2)	1/2	0.9113(2)	0.122(1)
N1	0.798(1)	1/2	1.070(2)	0.14(1)
N1A	0.831(1)	1/2	1.134(2)	0.13(1)
C1	0.841(1)	0.558(2)	1.053(2)	0.15(1)
C2	0.897(1)	1/2	1.035(2)	0.19(1)
C3	0.925(1)	0.409(3)	1.007(3)	0.21(1)
N2	0.532(1)	1/2	0.362(1)	0.08(1)
C4	0.521(1)	0.562(2)	0.242(1)	0.10(1)
C5	0.546(1)	0.450(2)	0.178(2)	0.14(1)
C6	0.590(1)	0.555(4)	0.142(2)	0.16(1)
N3	0.823(1)	1/2	0.466(1)	0.11(1)
C7	0.838(1)	0.541(3)	0.581(1)	0.10(1)
C8	0.901(1)	0.467(2)	0.655(1)	0.11(1)
C9	0.950(1)	1/2	0.653(2)	0.17(1)

Table 4. Final atomic coordinates and equivalent isotropic displacement parameters (Å$^2 \cdot 10^3$) for non-H atoms for the (C$_3$H$_5$NH$_3$)$_3$[BiCl$_6$] structure at 200 K ($C2/c$).

Atom	x	y	z	U_{eq}
Bi1	0.8977(1)	0.7334(1)	0.3210(1)	0.0326(1)
Cl1	0.9433(1)	0.4964(2)	0.2742(1)	0.0444(4)
Cl1A	0.9269(1)	0.9766(2)	0.2586(1)	0.0533(4)
Cl2A	0.8759(1)	0.4822(2)	0.3840(1)	0.0481(4)
Cl2	0.8545(1)	0.9737(2)	0.3622(1)	0.0555(4)
Cl3	1.0063(1)	0.7955(2)	0.4386(1)	0.0444(3)
Cl4	0.7963(1)	0.6867(2)	0.2037(1)	0.0619(4)
N1	1.218(1)	0.287(1)	0.264(1)	0.06(1)
C1	1.201(1)	0.217(3)	0.311(1)	0.11(1)
C2	1.237(1)	0.225(2)	0.382(1)	0.09(1)
C3	1.262(1)	0.119(2)	0.433(1)	0.12(1)
N1A	1.184(1)	0.248(2)	0.266(1)	0.07(1)
C1A	1.237(1)	0.161(2)	0.319(1)	0.07(1)
C2A	1.236(2)	0.138(3)	0.379(1)	0.10(1)
C3A	1.232(2)	0.254(4)	0.415(2)	0.17(1)
N2	1.0657(2)	0.735(1)	0.3524(2)	0.045(1)
C4	1.1213(3)	0.663(1)	0.4064(4)	0.073(2)
C5	1.1635(3)	0.776(1)	0.4520(5)	0.095(3)
C6	1.1827(4)	0.807(1)	0.5151(4)	0.112(3)
N3	0.979(1)	0.214(2)	0.407(1)	0.048(1)
C7	1.032(1)	0.306(3)	0.440(1)	0.06(1)
C8	1.082(1)	0.212(2)	0.437(1)	0.06(1)
C9	1.077(1)	0.208(2)	0.377(1)	0.07(1)
C7A	1.044(1)	0.258(3)	0.455(2)	0.06(1)
C8A	1.064(1)	0.233(3)	0.400(1)	0.05(1)
C9A	1.114(1)	0.166(2)	0.430(1)	0.08(1)

in the phase transition at 299 K. Therefore the X-ray investigations have been performed at 200 and 315 K.

In both phases the crystals are monoclinic. At 200 K the space group is $C2/c$ whereas at 315 K it is $C2/m$.

Table 5. Comparison of selected bond lengths/Å and angles/°
for $(C_3H_5N_3)_3[BiCl_6]$ at 315 and 200 K.

	315 K	200 K
Bi1–Cl1	2.731(1)	2.748(1)
Bi1–Cl1^I (Cl1A)	2.731(1)	2.731(1)
Bi1–Cl2	2.649(1)	2.648(1)
Bi1–Cl2^I (Cl2A)	2.649(1)	2.675(1)
Bi1–Cl3	2.759(2)	2.773(1)
Bi1–Cl4	2.638(2)	2.646(2)
Cl1–Bi1–Cl1^I(Cl1A)	87.79(7)	87.33(4)
Cl1–Bi1–Cl2	176.47(5)	177.08(5)
Cl1^I(Cl1A)–Bi1–Cl2^I (Cl2A)	176.47(5)	175.80(5)
Cl1–Bi1–Cl2^I (Cl2A)	89.24(5)	89.09(4)
Cl1–Bi1–Cl3^I	81.55(8)	90.08(4)
Cl1– Bi1–Cl3	92.02(8)	
Cl1^I(Cl1A)–Bi1–Cl3^I	92.06(7)	84.36(4)
Cl1^I(Cl1A)–Bi1–Cl3	81.63(7)	
Cl1–Bi1–Cl4	91.40(6)	89.01(5)
C2^I(Cl2A)–Bi1–Cl4	90.57(6)	90.33(5)
Cl2–Bi1–Cl1^I(Cl1A)	89.24(5)	89.79(5)
Cl2–Bi1–Cl2^I(C2A)	93.67(7)	93.80(5)
Cl2^I (Cl2A)–Bi1–Cl3^I	85.62(7)	93.44(4)
Cl2^I (Cl2A)–Bi1–Cl3	96.59(7)	
Cl2–Bi1–Cl3^I	96.59(7)	90.12(4)
Cl2–Bi1–Cl3	85.62(7)	
Cl2–Bi1–Cl4	90.57(6)	90.60(5)
Cl3^I–Bi1–Cl4	172.09(5)	176.10(4)
Cl3–Bi1–Cl4	172.09(5)	
Cl4–Bi1–Cl1^I (Cl1A)	91.40(6)	91.81(5)

Symmetry code: (^{I}) $x, -y+1, z$.

Table 6. The strongest H-bonds/Å,° for $(C_3H_5N_3)_3[BiCl_6]$ at 315 and 200 K.

D–H...A	D–H	H...A	D...A	D–H...A
		315 K		
N1–H1A...Cl4	0.89	2.65	3.07(2)	110
N1A–H1B...Cl2^{I*}	0.89	2.61	3.33(2)	139
N2–H2A...Cl1^{II*}	0.89	2.45	3.248(5)	149
N2–H2B...Cl3*	0.89	2.34	3.223(7)	171
		200 K		
N1–H1A...Cl2A^{III}	0.89	2.58	3.291(9)	137
N1–H1B...Cl4^{IV}	0.89	2.49	3.210(9)	138
N1–H1C...Cl4^{III}	0.89	2.48	3.281(9)	150
N2–H2B...Cl1A^{III}	0.89	2.33	3.220(4)	174
N2–H2C...Cl3	0.89	2.38	3.176(4)	148
N3–H3B...Cl3^V	0.89	2.54	3.355(4)	152
N3–H3C...Cl1A^V	0.89	2.62	3.390(4)	146

* One of the two symmetry related conections is given. Symmetry codes: (^{I}) $3/2-x, 3/2-y, 2-z$; (^{II}) $1-x, y, 1-z$; (^{III}) $2-x, y, 1/2-z$; (^{IV}) $1/2+x, -1/2+y, z$; (^{V}) $x, -1+y, z$.

At both temperatures the structures are composed of $[BiCl_6]^{3-}$ octahedra and allylammonium cations attracted to each other by N–H...Cl hydrogen bonds. Turel *et al.* indicated that such isolated $[BiCl_6]^{3-}$ anions are not very common [1]. In the Cambridge Structural Database [7], among all the fifty-nine chlorobismuthate(III) entries there are nineteen compounds
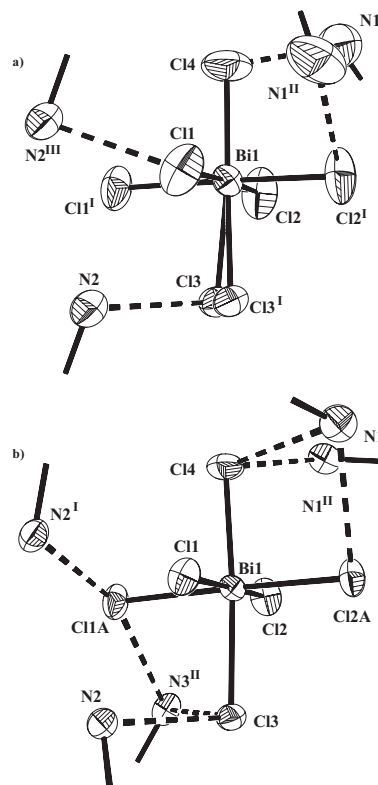

Fig. 2. Comparison of the environment of the $[BiCl_6]^{3-}$ octahedra in the structure of $(C_3H_5NH_3)_3[BiCl_6]$ at 315 K (a) and 200 K (b). For atoms N2, N1^{II}, N2^{III} one of the two symmetry related atoms are given. Only the strongest hydrogen bonds are shown. Displacement ellipsoids are plotted at the 50% probability level. Symmetry codes: (a) (^{I}) $x, -y+1, z$; (^{II}) $-x+1.5, -y+1.5, -z+2$; (^{III}) $-x+1, y, -z+1$; (b) (^{I}) $-x+2, y, -z+0.5$; (^{II}) $x, y-1, z$.

in which anionic substructures are built of isolated $[BiCl_6]^{3-}$ octahedra.

2.2.1. Structure at 315 K

The geometry of the hexachlorobismuthate(III) ion is distorted, the Cl–Bi–Cl bond angles are in the ranges: $81.55(8)-96.59(7)°$ for *cis* and $172.09(6)-176.47(5)°$ for *trans*. The Bi–Cl distances, ranging from 2.639(3) to 2.760(3) Å, are as expected and they are in a good agreement with the values found for other hexachlorobismuthates(III) (Table 5) [2, 3].

One out of six Cl ligands in the coordination sphere of the central Bi^{III} atom is disordered, with the Cl3 atom on two sites with equal occupancy. The distortion of $[BiCl_6]^{3-}$ octahedra is due to the extended and complex network of hydrogen bonds between the N atoms of the organic cations and the halogens of the
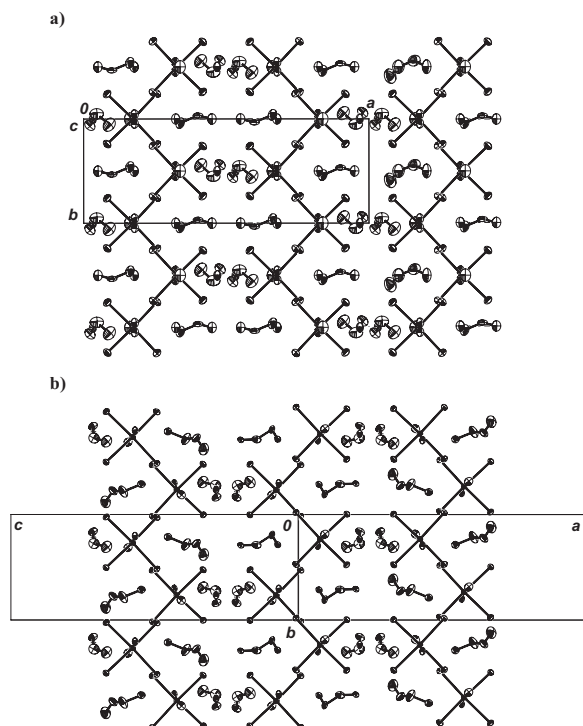
a)

b)

Fig. 3. Packing diagrams of the $(C_3H_5NH_3)_3[BiCl_6]$ molecule at 315 K (a) and 200 K (b). Displacement ellipsoids are plotted at the 25% probability level.

inorganic substructure. These hydrogen bonds diminish the charge density at the halide atoms and minimize ligand-ligand repulsions [1]. The geometry of $[BiCl_6]^{3-}$ and the hydrogen bonding pattern indicate that the distortion of the $[BiCl_6]^{3-}$ octahedra depends more on the hydrogen bonds rather than on the lone electron pair repulsion. These effects were also discussed in earlier papers by Lazarini [8, 10].

The hydrogen bonds change the geometry of $[BiCl_6]^{3-}$ octahedra, the Bi–Cl bond lengths as well as Cl–Bi–Cl angles. Thus the Bi1–Cl1 (Bi1–Cl1^I, 2.731(1) Å) and Bi1–Cl3 (2.759(2) Å) bonds are elongated while the remaining Bi1–Cl2 (Bi1–Cl2^I, 2.649(1) Å) and Bi–Cl4 bonds (2.638(2) Å) located *trans* are shortened (Table 5). The N1^{II}–H1B^{II}...Cl2 hydrogen bond causes an increase of the Cl2–Bi1–Cl2^I angle (93.67(7)°), whereas N2^{III}–H2A^{III}...Cl1 causes the decrease of the Cl1–Bi1–Cl1^I angle (87.79(7)°) (Fig. 2, Table 6). Furthermore the N1–H1A...Cl4 interaction leads to changes in the Cl1–Bi1–Cl4 and Cl1^I–Bi1–Cl4 angles.

There are three crystallographically independent allylammonium cations in the structure. All of them are

disordered. The atoms C1, C3, C4, C5, C6, C7 and C8 are split between two positions with occupancy factors of 0.5. The bond lengths and angles within the $(C_3H_5NH_3)^+$ cations were determined with low accuracy.

2.2.2. Structure at 200 K

At 200 K the title salt crystallizes in the monoclinic space group $C2/c$. All chlorine atoms are in the general positions. The central Bi^{III} atom is surrounded by six crystallographically independent chlorine ligands, which form a distorted $[BiCl_6]^{3-}$ octahedron. The atom Cl3 is ordered. The arrangement of the chloro ligands around the central Bi^{III} atom at 200 K deviates less from the ideal octahedron than in the 315 K phase. Three *trans* Cl–Bi–Cl angles are between 175.80(5) and 177.08(5)° and twelve *cis* angles range from 84.36(4) to 93.80(5)°. There are three *trans* pairs of Bi–Cl distances in the distorted $[BiCl_6]^{3-}$ octahedron: Bi1–Cl1 *vs.* Bi1–Cl2, Bi1–Cl1A *vs.* Bi1–Cl2A, Bi1–Cl3 *vs.* Bi1–Cl4. The main difference between distortions of the $[BiCl_6]^{3-}$ octahedra at both temperatures lies in the fact, that the atom Cl3 is disordered at 315 K. Its mean position at 315 K corresponds well to its position at 200 K. The largest deviation between the Bi–Cl bond lengths, 0.026(2) Å, at both temperatures was found for the Bi1–Cl2^I (Cl2A) distance (Table 5). This deviation corresponds to the presence of the slightly different N1A–H1B...Cl2^I (N1–H1A...Cl2A^I) interactions (Table 6).

The elongation of any particular Bi–Cl bond and the shortening of the distance opposite is a results of two effects. The first one, the so-called *trans*-influence, suggests that any elongation of a Bi–Cl bond leads to a shortening of the opposite bond length. The second stems from N...Cl interactions between the oppositely charged organic and inorganic sublattices. In all cases one of the Bi–Cl bond length is increased and another one located opposite, at the same time, is decreased. Additionally, all Cl atoms (Cl1, Cl1A and Cl3) involved in the elongation of Bi–Cl distances are linked by hydrogen bonds to the organic sublattice. This strong influence of a hydrogen bonding network on the inorganic polyhedra was also observed in other studies devoted to halogenobismuthates(III) [9, 10, 12, 13]. The most significant differences between the opposite bond lengths are 0.121(2) Å at 315 K and 0.127(2) Å at 200 K for Bi1–Cl3 and Bi1–Cl4, respectively. They are a consequence of the particularly strong N–H...Cl3

interactions (Table 6). Concurrently, the atom Cl4 is involved in rather weak hydrogen bonds. This effect was also described by Benetollo *et al.* [14].

2.3. Phase transition

The phase transition at 299 K is attributed to the ordering of one crystallographically independent allylammonium cation (Fig. 4), which lies on the special position of the plane *m* (at 315 K). Above the phase transition temperature the allylammonium cation is reoriented along its long axis, while below 299 K the motions are frozen. As a result of the phase transition the mirror plane *m* is replaced by a glide plane *c*. The *C*2/*m* space group changes therefore into the *C*2/*c* at the temperature of the phase transition. This corresponds to a *klassengleiche* symmetry reduction of index 2 from *C*2/*m* to *C*2/*c* upon doubling of one subcell axes.

The changes in the molecular dynamics of allylammonium cations are also reflected in the geometrical changes of the N–H...Cl hydrogen-bonding system. It seems that the remaining two organic cations are disordered in almost the same manner at both temperatures. At higher temperature the carbon atoms C2 and C9 are ordered while in the low-temperature phase they are disordered. The disorder of the cations N1 and N3 is realized by the presence of two positions for all C atoms and N1 atom with occupancy factors of 0.6 and 0.4.
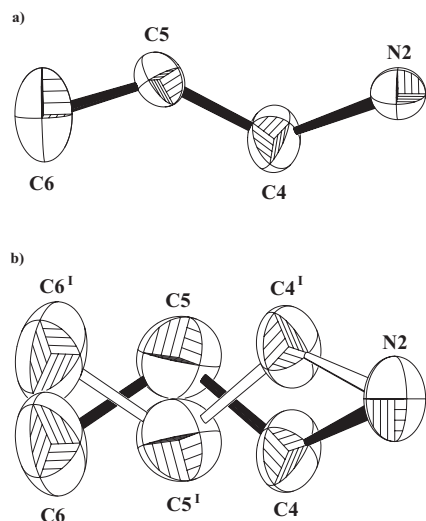

Fig. 4. Comparison of the corresponding allylammonium cations in the structure of (C$_3$H$_5$NH$_3$)$_3$[BiCl$_6$] at 200 K (a) and 315 K (b). Displacement ellipsoids are plotted at the 25% probability level. Symmetry code: ($^{\rm I}$) *x*, −*y* + 1, *z*.

3. Conclusions

Tris(allylammonium) hexachlorobismuthate(III) undergoes three phase transitions at 152, 191 and 299 K. All of them are most probably of the order-disorder type. The structure of the (C$_3$H$_5$NH$_3$)$_3$[BiCl$_6$] salt was studied at 200 and 315 K, by single-crystal X-ray diffraction. At both temperatures the compound crystallizes in monoclinic centrosymmetric space groups. The same anionic substructures, built of the distorted [BiCl$_6$]$^{3-}$ octahedra, were found in both phases. The distortions of the anionic substructures are mainly related to the difference in strength of the N–H...Cl interactions between the oppositely charged anionic and cationic substructures. The mechanism of the phase transition at 299 K is related to the ordering of one of the three non-equivalent allylammonium cation located at a special position in the lower temperature phase. The consequence of the cation ordering process is a change in the lattice symmetry – the mirror plane *m* transforms into the glide plane *c*.

4. Experimental Section

Tris(allylammonium) hexachlorobismuthate(III) was obtained in the reaction of allylamine and basic bismuth(III) carbonate in an aqueous solution of hydrochloric acid. Single crystals suitable for X-ray diffraction studies were grown by slow evaporation of solvent at room temperature. At both temperatures measurements were performed on a Xcalibur single crystal diffractometer equipped with the Oxford Cryosystems cooler. The *ω-scan* technique was used. For all data Lorentz, polarisation and empirical absorption corrections based on the symmetry equivalent reflections [15] were performed ($T_{\min} = 0.100$, $T_{\max} = 0.211$ for the structure at 315 K and $T_{\min} = 0.150$, $T_{\max} = 0.283$ for the structure at 200 K).

Both structures were solved by the Patterson method. The positions of the hydrogen atoms in the structures were refined using a riding model. The hydrogen atoms were added to all C and N atoms of the ordered cation (structure at 200 K) and to the N atoms only in the case of the disordered ones (structures at 200 and 315 K). The details of data collection and refinement are listed in Table 2. For all non-hydrogen atoms anisotropic displacement parameters were refined.

The quantity minimised was $\Sigma w(|F_{\rm o}| - |F_{\rm c}|)^2$ with the weighting scheme $w = 1/[\sigma^2(F_{\rm o}^2) + (0.0139P)^2]$ and $w = 1/[\sigma^2 F_{\rm o}^2) + (0.0325P)^2](P = (F_{\rm o}^2 + 2F_{\rm c}^2)/3)$ at 200 and 315 K, respectively.

CrysAlis programs [16] were used in the cell refinement, data collection and data reduction processes. The SHELXS-97, SHELXL-97 [17] and SHELXTL [15] programs were

used for structure solutions, refinements and structure drawings.

The TGA measurements were carried out with a heating rate of 10 K·min^{-1} in the temperature range 270 – 770 K on a TGA 2050 TA Instruments apparatus.

The DSC analyses were performed using a DSC 2010 TA Instruments calorimeter with cooling/heating rates of 10 K·min^{-1}. The measurements were performed in the temperature range 130 – 310 K.

Crystallographic data (excluding structure factors) for tris(allylammonium) hexachlorobismuthate(III) at 200 and 315 K have been deposited at the Cambridge Crystallographic Data Centre as supplementary publication nos. CCDC 237508 and CCDC 237509, respectively. Copies of the data *ca.* be obtained, free of charge, on application to the Director, CCDC, 12 Union Road, Cambridge CB2 1EZ, UK (Fax: int. code+(1223) 336033 or e-mail: data_request@ccdc.cam.ac.uk).

[1] L. P. Battaglia, A. Bonamartini Corradi, Inorg. Chim. Acta **121**, 1431 (1986).

[2] I. Turel, I. Leban, N. Bukovec, J. Inorg. Biochem. **66**, 241 (1997).

[3] F. Benettolo, G. Bombieri, G. Alonzo, N. Bertazzi, G. A. Cassela, J. Chem. Crystallogr. **28**, 791 (1998).

[4] P. Ciąpała, R. Jakubas, G. Bator, J. Zaleski, A. Pietraszko, M. Drozd, J. Baran, J. Phys. Condens. Matter **9**, 627 (1997).

[5] P. Carpentier, J. Lefebrve, R. Jakubas, Acta Crystallogr. **B51**, 167 (1995).

[6] R. Jakubas, L. Sobczyk, J. Lefebrve, Ferroelectrics **100**, 143 (1989).

[7] F. H. Allen, Acta Crystallogr. **B58**, 380 (2002). The Cambridge Structural Database: a quarter of a million crystal structures and rising, ver. 5.25 (November 2003).

[8] F. Lazarini, Acta Crystallogr. **C43**, 637 (1987).

[9] G. C. Papavassiliou, I. B. Koutselas, A. Terzis, C. P. Raptopoulou, Z. Naturforsch. **50b**, 1566 (1995).

[10] F. Lazarini, Acta Crystallogr. **C41**, 1617 (1985).

[11] R. Blachnik, B. Jaschinski, H. Reuter, G. Kaster, Z. Kristallogr. **212**, 874 (1997).

[12] S. Jarraya, A. Ben Salah, A. Daoud, Acta Crystallogr. **C49**, 1594 (1993).

[13] E. Herdtweck, U. Kreusel, Acta Crystallogr. **C49**, 318 (1993).

[14] F. Benetollo, G. Bombieri, A. Del Pra, G. Alonzo, N. Bertazzi, Inorg. Chim. Acta **319**, 49 (2001).

[15] G. M. Sheldrick, SHELXTL. Siemens Analytical X-ray Instrument Inc., Madison, Winsconsin, USA (1990).

[16] Oxford Diffraction; CrysAlis CCD, Data collection GUI for CCD and CrysAlis RED, CCD data reduction GUI versions 1.169.5 and 1.170.16, Oxford Diffraction Poland (2002).

[17] G. M. Sheldrick, SHELX-97. Program for the Solution and the Refinement of Crystal Structures. University of Göttingen, Germany (1997).